

Numerical Solutions of Open String Field Theory in Marginally Deformed Backgrounds

Isao KISHIMOTO¹ and Tomohiko TAKAHASHI²

¹*Faculty of Education, Niigata University,
Niigata 950-2181, Japan*

²*Department of Physics, Nara Women's University,
Nara 630-8506, Japan*

June, 2013

Abstract

We investigate numerical solutions of bosonic open string field theory in some marginally deformed backgrounds, which are obtained by expanding the action around an identity-based marginal solution with one parameter. We construct numerical solutions in the Siegel gauge and the Landau gauge corresponding to the tachyon vacuum. Their vacuum energy approximately cancels the D-brane tension for larger intervals of the parameter with increasing truncation level. The result is consistent with the previous expectation that the identity-based marginal solution has vanishing energy regardless of the values of the parameter. We also study the marginal branch (M -branch) and the vacuum branch (V -branch) and evaluate not only the vacuum energy but also the gauge invariant overlaps with the graviton and the closed tachyon. We observe that there is a finite bound for the value of the massless field of numerical solutions even in the marginally deformed background.

1 Introduction

Open bosonic string field theory has a non-perturbative vacuum corresponding to a marginal deformation such as background Wilson lines [1]. The effective potential of the massless field becomes increasingly flat as the truncation level is increased. On the analytical side, there are classical solutions expected to represent marginal deformations. As such solutions, identity-based marginal solutions were constructed in [2, 3, 4]. Furthermore, other types of marginal solutions have been constructed [5, 6, 7, 8]. The vacuum energies of these solutions are formally proved to be zero by differentiating and integrating the action with respect to a deformation parameter. However, it may be provided as a sort of indefinite quantity, especially in the case of identity-based solutions.

The tachyon vacuum exists even in the presence of Wilson lines, and the vacuum energy is expected to cancel the D-brane tension, which is equivalent to that of no Wilson lines. If we expand the string field around an analytic solution corresponding to background Wilson lines, the action for the fluctuation describes strings on the Wilson line background. Accordingly, the expanded theory should have a non-perturbative vacuum, the vacuum energy of which is given as the same one without Wilson lines. Actually, analytic tachyon vacuum solutions in the theory expanded around identity-based marginal solutions have been constructed in [9] using the “ $K'Bc$ algebra” and it is shown that their vacuum energy cancels a D-brane tension. This provides evidence that the vacuum energy of the identity-based marginal solutions is zero.

Here, we construct numerical tachyon vacuum solutions, which satisfy other gauge conditions: the Siegel gauge and the Landau gauge, using the level truncation method in the theory around an identity-based marginal solution with one real parameter x . We find that their vacuum energy approximately cancels the value of a D-brane tension for larger intervals of the parameter with increasing level.¹ The result is consistent with that of the analytic approach in [9] and implies that the energy of the identity-based marginal solution vanishes.

In [1], it was observed that there are two branches for an effective potential of a constant mode of the massless field, denoted as a_s , with the level truncation approximation. One is a “marginal branch” (M -branch), which includes the trivial zero solution, and the other is a “vacuum branch” (V -branch), which includes the tachyon vacuum solution. With increasing level, the shape of the M -branch becomes flatter. However, at a finite value of a_s , the M -branch and the V -branch merge and there is a maximum value of a_s for the M -branch. Recently, such a phenomenon was also observed for further higher level computations in [10]. In this context, we investigate the M -branch and the V -branch in the theory around the identity-based marginal solution. We find that the graph of the potential moves to the horizontal direction for small values of the parameter $|x|$. As for the V -branch, we observe that the value of $|a_s|$ at the potential minimum has a finite bound around 0.3. On the other hand, the M -branch seems to be unstable for large values of $|x|$.

We evaluate not only the vacuum energy as mentioned above but also gauge invariant overlaps with the graviton and the closed tachyon for the numerical solutions obtained. For the tachyon vacuum (the minimum of the V -branch) in the theory around the identity-based marginal solution, we find that, with increasing level, the gauge invariant overlap with the

¹ Precisely, in the Landau gauge, the numerical behavior may not be stable for large $|x|$.

graviton approaches 1 for various values of x but that with the closed tachyon approaches e^{-4ix} . On the other hand, for the M -branch in the original theory, the gauge invariant overlap with the graviton approaches 0 for various values of a_s but that with the closed tachyon depends on a_s , such as $1 - e^{-ica_s}$ with some constant c approximately.

This paper is organized as follows. In §2, we will construct numerical solutions, both in the Siegel and Landau gauges, in the theory expanded around an identity-based marginal solution with one parameter x , and evaluate their gauge invariants. In §3, we will discuss the M -branch and V -branch in the expanded theory for various values of x . In §4, we will comment on the gauge invariant overlaps with the graviton and the closed tachyon for numerical solutions in the M -branch. In §5, we will give some concluding remarks. In appendix A, we will show some numerical results on the BRST invariance of the solutions.

2 Tachyon vacuum around an identity-based marginal solution

The equation of motion in open bosonic string field theory is given by $Q_B\Psi + \Psi * \Psi = 0$. As an analytic classical solution, we have a type of identity-based solution [2, 3, 4]:

$$\Psi_0 = - \int_{C_{\text{left}}} \frac{dz}{2\pi i} \frac{i}{2\sqrt{\alpha'}} F(z)c(z)\partial X^{25}(z)I + \frac{1}{4} \int_{C_{\text{left}}} \frac{dz}{2\pi i} F(z)^2c(z)I, \quad (2.1)$$

where I is the identity string field and $F(z)$ is a function that satisfies $F(-1/z) = z^2F(z)$. In the integrations, C_{left} denotes the path along a unit half circle such as $\text{Re } z \geq 0$. We can see that this solution corresponds to the Wilson line along the 25th direction from the study of the expanded theory around the solution. In this solution, the Wilson line parameter is involved as

$$f = \int_{C_{\text{left}}} \frac{dz}{2\pi i} F(z). \quad (2.2)$$

The usual Wilson line is proportional to this quantity. Other modes of the function can be gauged away [4].

Expanding the string field around the solution as $\Psi = \Psi_0 + \Phi$, we can find the action $S'[\Phi]$ for the fluctuation around the Wilson line background:

$$S'[\Phi] \equiv S[\Psi_0 + \Phi] - S[\Psi_0] = - \left(\frac{1}{2} \langle \Phi, Q'\Phi \rangle + \frac{1}{3} \langle \Phi, \Phi * \Phi \rangle \right). \quad (2.3)$$

The modified BRST operator in the expanded action is given by

$$Q' = Q_B - \oint \frac{dz}{2\pi i} \frac{i}{2\sqrt{\alpha'}} F(z)c(z)\partial X^{25}(z) + \frac{1}{4} \oint \frac{dz}{2\pi i} F(z)^2c(z), \quad (2.4)$$

where Q_B denotes the original BRST operator and the integration contour is along the unit circle. In the following, we take a function $F(z)$ as $F(z) = -x(z + 1/z)z^{-1}$ for simplicity,

where x is a real parameter. Then, (2.4) is explicitly written as

$$Q' = Q_B + \frac{x}{\sqrt{2}} \sum_{n \in \mathbb{Z}} c_n (\alpha_{-n-1}^{25} + \alpha_{-n+1}^{25}) + \frac{x^2}{4} (2c_0 + c_{-2} + c_2). \quad (2.5)$$

With respect to the above Q' , we solve the equation of motion:

$$Q'\Phi + \Phi * \Phi = 0, \quad (2.6)$$

numerically.

First of all, we construct the tachyon vacuum solution in the Siegel and Landau gauges, which corresponds to the analytic solution constructed by the method of $K'Bc$ algebra in [9]:

$$\Phi_T = \frac{1}{\sqrt{1+K'}} (c + cK'Bc) \frac{1}{\sqrt{1+K'}}, \quad (2.7)$$

which satisfies the other gauge condition.² To construct a numerical solution to the equation of motion (2.6) with a gauge condition, we solve

$$\mathcal{P}_1 \Phi = 0, \quad (2.9)$$

$$\mathcal{P}_2 (Q'\Phi + \Phi * \Phi) = 0, \quad (2.10)$$

for Φ . \mathcal{P}_1 and $\mathcal{P}_2 = 1 - \text{bpz}(\mathcal{P}_1)$ are projections determined by a gauge condition. In the case of the Siegel gauge, these are given by

$$\mathcal{P}_1 = \mathcal{P}_2 = c_0 b_0, \quad (2.11)$$

and, in the case of the Landau gauge [12, 13], these are³

$$\mathcal{P}_1 = -\left(c_0 + \frac{\tilde{Q}}{L_0}\right) b_0 c_0 W_1 \tilde{Q}, \quad \mathcal{P}_2 = \left(c_0 + \frac{\tilde{Q}}{L_0}\right) \left(b_0 \left(1 + \frac{1}{L_0} \tilde{Q} W_1 \tilde{Q}\right) - b_0 c_0 \tilde{Q} W_1\right), \quad (2.12)$$

where \tilde{Q} is given by ghost zero mode expansion of Q_B :

$$Q_B = c_0 L_0 + b_0 M + \tilde{Q} \quad (2.13)$$

and W_1 is defined by

$$W_1 = \sum_{k=0}^{\infty} \frac{(-1)^k}{((k+1)!)^2} M^k (M^-)^{k+1}, \quad M^- \equiv -\sum_{k=1}^{\infty} \frac{1}{2k} b_{-k} b_k. \quad (2.14)$$

² It satisfies a kind of “dressed \mathcal{B}_0 gauge” condition [11]:

$$\frac{1}{\sqrt{1+K'}} \left[(\mathcal{B}_0 - \mathcal{B}_0^\dagger) \left(\sqrt{1+K'} \Phi_T \sqrt{1+K'} \right) \right] \frac{1}{\sqrt{1+K'}} = 0. \quad (2.8)$$

³ For the ghost number 1 string fields, the condition $\mathcal{P}_1 \Phi = 0$ can be rewritten as $b_0 c_0 \tilde{Q} \Phi = 0$. The Siegel gauge and the Landau gauge are interpolated by one real parameter, called the a -gauge [12].

2.1 On the level truncation method

In order to perform numerical calculations, we restrict ourselves to the subspace spanned by the following basis.

- We consider only the zero momentum sector with the ghost number 1.
- In the matter sector, except for the 25th direction, we use only the Virasoro generator with the central charge $c = 25$, denoted as $L_{-n}^{(m)'} (n > 1)$.
- As for the 25th sector, we use the conventional oscillator $\alpha_{-n}^{25} (n \geq 1)$.
- In the ghost sector, we use $b_{-n} (n > 0)$, $c_{-n} (n \geq 0)$ on $c_1|0\rangle$, where $|0\rangle$ is the conformal vacuum.
- We take the even Ω' sector with $\Omega' \equiv (-1)^{L_0+1} P_{25} [1]$, where P_{25} is a parity transformation with respect to the 25th direction such as $P_{25}\alpha_{-n}^{25}(P_{25})^{-1} = -\alpha_{-n}^{25}$, $P_{25}|0\rangle = |0\rangle$.

Using the above conditions, a general form of the basis is

$$L_{-n_1}^{(m)'} L_{-n_2}^{(m)'} \cdots L_{-n_l}^{(m)'} \alpha_{-m_1}^{25} \alpha_{-m_2}^{25} \cdots \alpha_{-m_a}^{25} b_{-k_1} b_{-k_2} \cdots b_{-k_b} c_{-l_1} c_{-l_2} \cdots c_{-l_b} c_1 |0\rangle, \quad (2.15)$$

$$n_1 \geq \cdots n_l \geq 2, \quad m_1 \geq \cdots m_a \geq 1, \quad k_1 > \cdots k_b \geq 1, \quad l_1 > \cdots l_b \geq 0, \quad (2.16)$$

$$n_1 + \cdots n_l + m_1 + \cdots m_a + k_1 + \cdots k_b + l_1 + \cdots l_b + a = \text{even}. \quad (2.17)$$

In fact, a space spanned by the above basis is closed under the action of the operator (2.5) and the star product and it is consistent with the Siegel and Landau gauge condition.

Furthermore, we use the $(L, 3L)$ -truncation method with respect to the level associated with L_0 . Namely, string fields are truncated up to the level L , which is an eigenvalue of $L_0 + 1$, and each term of the expansion of the star product of string fields is truncated up to the total level $3L$.

Concretely, the dimension of the truncated space as above is N_L in Table 1 and M_L is that of the space where the Siegel or Landau gauge condition is imposed.

L	0	1	2	3	4	5	6	7	8
N_L	1	2	6	12	29	56	118	218	420
M_L	1	2	5	9	20	37	75	135	255
L	9	10	11	12	13	14	15	16	...
N_L	745	1348	2307	3985	6614	11011	17799	28764	...
M_L	446	797	1351	2315	3817	6317	10161	16346	...

Table 1: Dimensions of the truncated space for the level L .

To solve (2.9), (2.10) numerically, we use Newton's method. With an appropriate initial configuration $\Phi_{(0)}$, we solve a set of linear equations:

$$\mathcal{P}_1 \Phi_{(n+1)} = 0, \quad (2.18)$$

$$\mathcal{P}_2(Q' \Phi_{(n+1)} + \Phi_{(n)} * \Phi_{(n+1)} + \Phi_{(n+1)} * \Phi_{(n)}) = \mathcal{P}_2(\Phi_{(n)} * \Phi_{(n)}), \quad (2.19)$$

iteratively in the truncated space. If $\lim_{n \rightarrow \infty} \Phi_{(n)}$ exists, it gives a solution to (2.9) and (2.10). Actually, for a fixed truncation level L , we terminate the iterative procedure if the relative error of the convergence reaches $\|\Phi_{(n+1)} - \Phi_{(n)}\|/\|\Phi_{(n)}\| < 10^{-8}$.

We construct the tachyon vacuum solutions in the Siegel gauge and the Landau gauge in the theory with Q' (2.5) as follows:

- We begin by constructing a solution in the case of $x = 0$ (the original theory with Q_B). We take $\Phi_{(0)} = \frac{64}{81\sqrt{3}}c_1|0\rangle$, which is a nontrivial solution in the lowest level truncation, as an initial configuration and then we get a converged solution $\Phi_{x=0}$, which is twist even, using the iterative procedure (2.18) and (2.19).
- In the case of a positive value of x , we use a converged configuration $\Phi_{x-\epsilon}$ in the theory of Q' with $x - \epsilon$ for a small value of $\epsilon (> 0)$ as an initial configuration. Solving (2.18) and (2.19) iteratively, we get a converged solution in the theory of Q' with x .
- In the case of a negative value of x , noting (2.5), a numerical solution can be obtained by the parity transformation with respect to the 25th direction from the solution in the theory of Q' with $-x$, namely, $\Phi_x = P_{25}\Phi_{-x}$.
- At large values of $|x|$, we reach the trivial solution $\Phi_x = 0$ using the above procedure.

It turns out that it takes 10 iterations or fewer to get each converged solution.

2.2 Evaluation of the vacuum energy

Here we demonstrate the results of the evaluation of the vacuum energy $E = V[\Phi_x]$ for the numerical solutions Φ_x obtained as in §2.1. We normalize the potential $V[\Phi]$ by a D-brane tension as

$$V[\Phi] = -2\pi^2 S'[\Phi] = 2\pi^2 \left(\frac{1}{2} \langle \Phi, Q' \Phi \rangle + \frac{1}{3} \langle \Phi, \Phi * \Phi \rangle \right). \quad (2.20)$$

Noting the relation $V[\Phi_x] = V[P_{25}\Phi_{-x}] = V[\Phi_{-x}]$, we consider only the case of nonnegative values of x .

In the case of the Siegel gauge, we have Fig. 1. For a fixed value of x , E approaches -1 with increasing truncation level and the region where $E \simeq -1$ becomes larger for higher levels. In the infinite level limit, it seems to be $E = -1$ for all values of x . Therefore, it is consistent that the numerical solutions Φ_x can be interpreted to represent the tachyon vacuum in the theory of Q' with x , where a D-brane vanishes.

In the case of the Landau gauge, we have Fig. 2.⁴ For a fixed value of x , E approaches -1 with increasing level up to $L = 4$. However, for $L = 5, 6, 7, 8$, we cannot find converged solutions for large $|x|$ with the same algorithm and the value of E seems to be unstable for $|x| > 2$ even if there exist numerical solutions. Compared to the result in the Landau gauge, the level truncation in the Siegel gauge might be suitable for large values of $|x|$.

⁴ At $x = 0$, the values of E are the same as in [14] for $L = 0, 2, 4, 6$ and they are slightly different from those in [15] because a different projection for (2.10) is adopted.

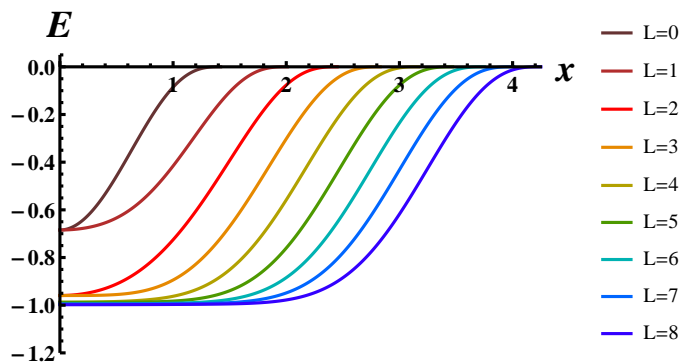


Figure 1: Plots of the vacuum energy $E = V[\Phi_x]$ (2.20) in the Siegel gauge for $L = 0, 1, 2, \dots, 8$ truncation.

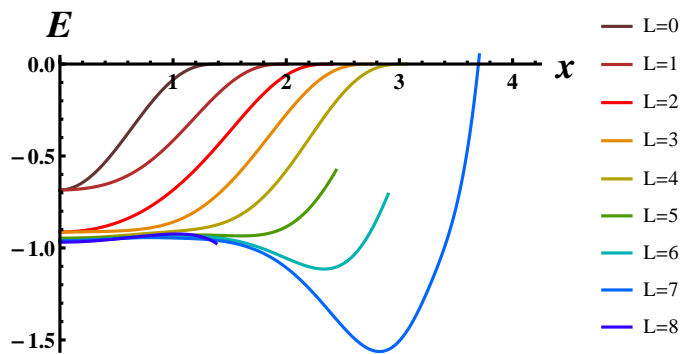


Figure 2: Plots of the vacuum energy $E = V[\Phi_x]$ (2.20) in the Landau gauge for $L = 0, 1, 2, \dots, 8$ truncation.

2.3 Evaluation of the gauge invariant overlaps

Here, we evaluate gauge invariant overlaps with the graviton and the closed tachyon for the numerical solutions Φ_x obtained as in §2.1. In general, the gauge invariant overlap $O_V(\Phi)$ is defined as

$$O_V(\Phi) = \langle I|V(i)|\Phi \rangle. \quad (2.21)$$

Here, $V(i)$ is given by $c\bar{c}V_m(z, \bar{z})$, where $V_m(z, \bar{z})$ is a vertex operator in the matter sector with the conformal dimension $(1, 1)$. (See [16] for details of explicit calculations.)

We evaluate the gauge invariant overlap with the graviton: $V_m \sim \partial X^0(i)\partial X^0(-i)$, where we denote (2.21) as $O_\zeta(\Phi)$, and the closed tachyon $V_m \sim e^{\frac{i}{2}k(X^{25}(i)-X^{25}(-i))}$ with $k^2 = 4/\alpha'$ for a Dirichlet direction, where we denote (2.21) as $O_k(\Phi)$. We normalize them as

$$O_\zeta(\Phi_T) = 1, \quad (2.22)$$

$$O_k(\Phi_T) = e^{-4ix} \quad (2.23)$$

for the analytic solution (2.7) using the result in [9, 17].

In the Siegel gauge, we have evaluated the gauge invariant overlap with the graviton for the tachyon vacuum solution in the theory of Q' with x as in Fig. 3. With increasing level, it approaches a constant near 1 for larger regions of x , which is the same value as in (2.22). Namely, in the infinite level limit, we expect $O_\zeta(\Phi_x) = 1$ for all x .

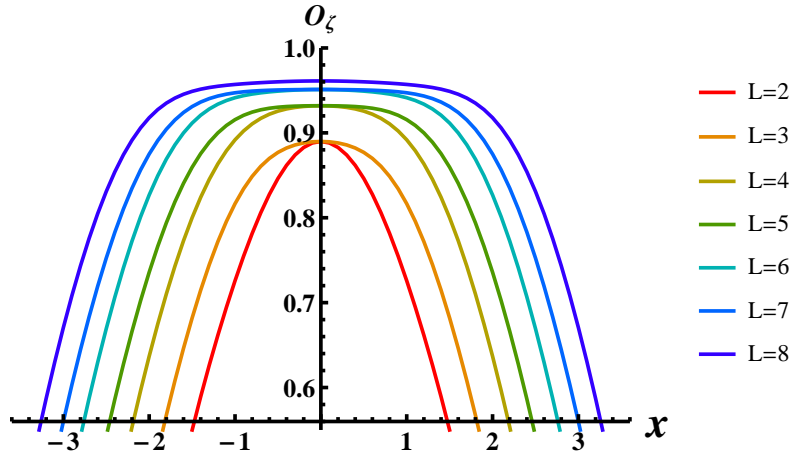


Figure 3: Plots of the gauge invariant overlap (2.21) with the graviton $O_\zeta(\Phi_x)$ in the Siegel gauge for the tachyon vacuum using $L = 2, 3, \dots, 8$ truncation.

The gauge invariant overlap with the closed tachyon for the tachyon vacuum solution in the theory of Q' with x is evaluated as in Fig. 4 for its real part, and Fig. 5 for its imaginary part.

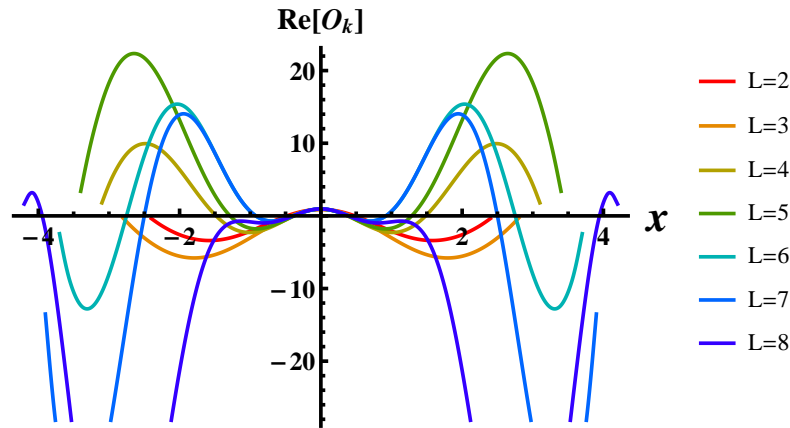


Figure 4: Plots of the real part of the gauge invariant overlap (2.21) with the closed tachyon $O_k(\Phi_x)$ in the Siegel gauge for the tachyon vacuum using $L = 2, 3, \dots, 8$ truncation.

At first sight, the plots of $O_k(\Phi_x)$ in Figs. 4 and 5 seem to be divergent for higher levels especially for large values of $|x|$. However, for small values of $|x|$, one can expect a structure

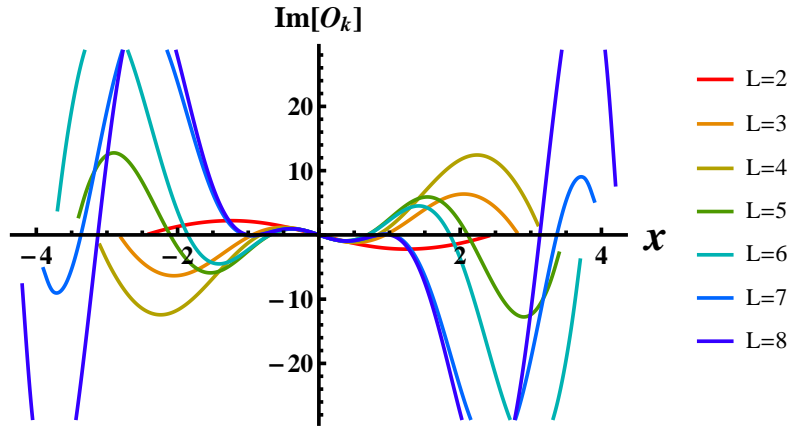


Figure 5: Plots of the imaginary part of the gauge invariant overlap (2.21) with the closed tachyon $O_k(\Phi_x)$ in the Siegel gauge for the tachyon vacuum using $L = 2, 3, \dots, 8$ truncation.

like (2.23). Actually, it seems to become $O_k(\Phi_x) \rightarrow e^{-4ix}$ with increasing truncation level, at least for small values of $|x|$ as in Figs. 6 and 7.

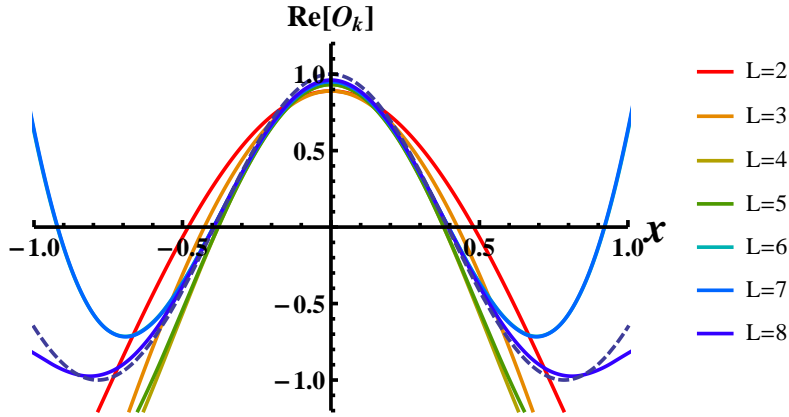


Figure 6: Superposition of Fig. 4 and $\cos 4x$ (dotted line) for small values of $|x|$.

3 M -branch and V -branch in the Q' -theory

In this section, we investigate the M -branch and the V -branch in the theory of Q' with x . Firstly, we consider them in the lowest level. In the $L = 1$ truncation, the string field Φ is expressed as

$$\Phi_{L=1} = t_0 c_1 |0\rangle + a_s \alpha_{-1}^{25} c_1 |0\rangle. \quad (3.1)$$

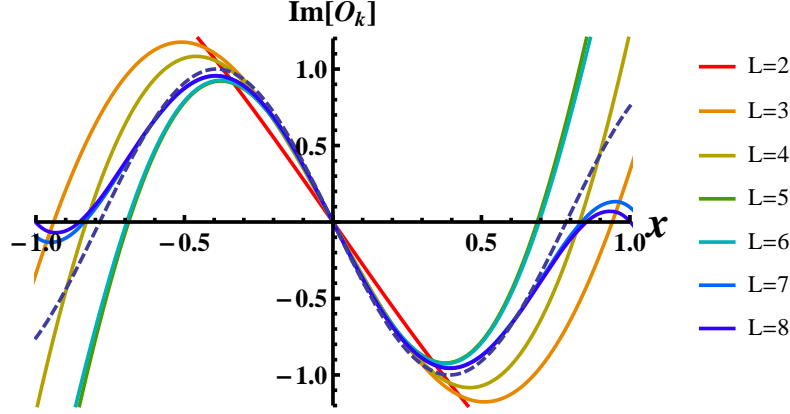


Figure 7: Superposition of Fig. 5 and $-\sin 4x$ (dotted line) for small values of $|x|$.

Substituting it into the action (2.3), we have

$$S'[\Phi_{L=1}] = \frac{t_0^2}{2} - \frac{x^2 t_0^2}{4} - \frac{x^2 a_s^2}{4} - \frac{x a_s t_0}{\sqrt{2}} - \frac{27\sqrt{3}}{64} t_0^3 - \frac{3\sqrt{3}}{4} a_s^2 t_0. \quad (3.2)$$

Solving $\frac{\partial}{\partial t_0} S'[\Phi_{L=1}] = 0$ with respect to t_0 , we have two solutions as functions of a_s :

$$t_0^{(\mp)}(a_s) = \frac{4}{81\sqrt{3}} \left(8 - 4x^2 \mp \sqrt{16(2-x^2)^2 - 162\sqrt{6}x a_s - 729a_s^2} \right). \quad (3.3)$$

One of them satisfies $t_0^{(-)}(a_s = 0) = 0$, which corresponds to the M -branch, and another one satisfies $t_0^{(+)}(a_s = 0) \neq 0$, which corresponds to the V -branch (for small values of $|x|$). Both of them exist only in a finite interval:

$$-\frac{\sqrt{2}}{27} \left(3\sqrt{3}x + \sqrt{32 - 5x^2 + 8x^4} \right) \leq a_s \leq \frac{\sqrt{2}}{27} \left(-3\sqrt{3}x + \sqrt{32 - 5x^2 + 8x^4} \right) \quad (3.4)$$

because of the reality of the tachyon field t_0 . At the end of the interval, the two branches merge.

Substituting $\Phi_{L=1}$ with these $t_0^{(\mp)}(a_s)$ (3.3) in $V[\Phi]$ (2.20), we obtain an effective potential as a function of a_s . For example, we have Figs. 8, 9, 10, 11, 12, 13 for the theory with $x = 0, -0.5, -1, -1.5, -2, -2.5$, respectively. The M -branch is depicted by $V_M(a_s) \equiv V[\Phi_{L=1}|_{t_0=t_0^{(-)}(a_s)}]$ and the V -branch is depicted by $V_V(a_s) \equiv V[\Phi_{L=1}|_{t_0=t_0^{(+)}(a_s)}]$. We find $V_M(a_s) \geq V_V(a_s)$ from explicit expressions.

In the case of $x^2 < 2$, we have expansions of two branches around $a_s = 0$ as

$$V_M(a_s) = \frac{\pi^2 x^2 (-4 + x^2)}{2(-2 + x^2)} a_s^2 + O(a_s^3), \quad V_V(a_s) = \frac{512\pi^2 (-2 + x^2)^3}{59049} + O(a_s). \quad (3.5)$$

Similarly, for $x^2 > 2$, we have

$$V_M(a_s) = \frac{512\pi^2 (-2 + x^2)^3}{59049} + O(a_s), \quad V_V(a_s) = \frac{\pi^2 x^2 (-4 + x^2)}{2(-2 + x^2)} a_s^2 + O(a_s^3). \quad (3.6)$$

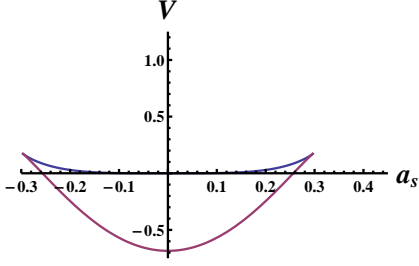


Figure 8: The M -branch and the V -branch for $L = 1$ in the original theory (i.e. $x = 0$).

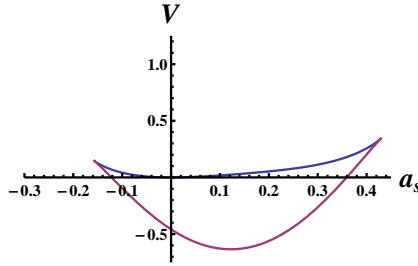


Figure 9: The M -branch and the V -branch for $L = 1$ in the theory with $x = -0.5$.

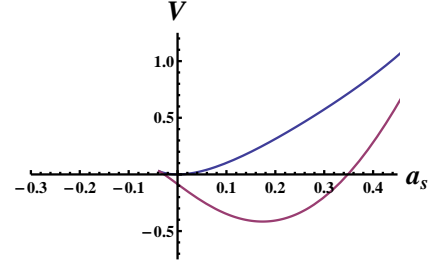


Figure 10: The M -branch and the V -branch for $L = 1$ in the theory with $x = -1$.

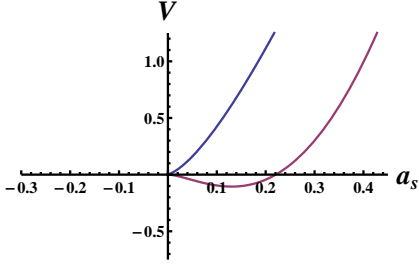


Figure 11: The M -branch and the V -branch for $L = 1$ in the theory with $x = -1.5$.

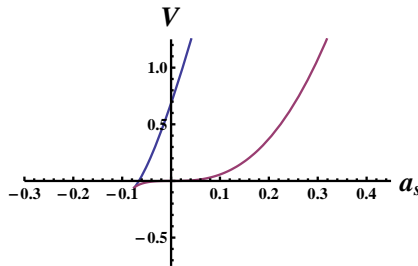


Figure 12: The M -branch and the V -branch for $L = 1$ in the theory with $x = -2$.

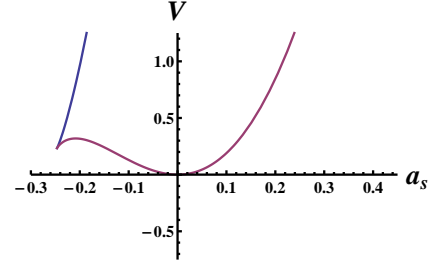


Figure 13: The M -branch and the V -branch for $L = 1$ in the theory with $x = -2.5$.

Therefore, we note that $V_V(a_s)$ has a second-order zero at $a_s = 0$ for $|x| > \sqrt{2}$.⁵ Actually, from Figs. 12 and 13, the graph of the V -branch for $|x| > \sqrt{2}$, given by $V_V(a_s)$, may be qualitatively similar to the “ M -branch” in the original theory.

For higher level truncation, we solve eqs. (2.9) and (2.10) with a fixed value of the massless field a_s using the iterative method with appropriate initial configurations. In a fixed level L truncation, for a fixed value of x , we take initial configurations as follows:

- For the V -branch, we begin from the value of a_s ($\equiv a_s^T$) of the tachyon vacuum solution constructed as in §2.1. Using the values of component fields of the tachyon vacuum except for a_s as an initial configuration, we solve eqs. (2.9) and (2.10) for $a_s = a_s^T \pm \varepsilon$ for a small value of ε (> 0). Then, we use the values of component fields of the converged solution with $a_s = a_s^T \pm \varepsilon$, except for a_s , as an initial configuration for the iteration

⁵ In the case of $|x| = \sqrt{2}$, both $V_M(a_s)$ and $V_V(a_s)$ become $O(a_s\sqrt{a_s})$ around $a_s = 0$.

with $a_s = a_s^T \pm 2\varepsilon$. Similarly, we use the configuration of the converged solution with $a_s = a_s^T \pm 2\varepsilon$ to solve (2.9) and (2.10) with $a_s = a_s^T \pm 3\varepsilon$, and so on.

- For the M -branch, we begin from the value of ε ($-\varepsilon$) for a_s and we use zeros for values of component fields except for a_s as an initial configuration to construct a solution of (2.9) and (2.10). Then, we use the values of the converged solution with $a_s = \varepsilon$ ($a_s = -\varepsilon$), except for a_s , as an initial configuration for the iteration with $a_s = 2\varepsilon$ ($a_s = -2\varepsilon$). Similarly, we use the configuration of the converged solution with $a_s = \pm 2\varepsilon$ to solve (2.9) and (2.10) with $a_s = \pm 3\varepsilon$, and so on.

We consider numerical solutions only in the Siegel gauge because it seems to be more stable than the Landau gauge, as seen in §2.2. All component fields can be expressed as functions of a_s numerically and we substitute them to the potential (2.20) to get an effective potential V_S as a function of a_s .

In the original theory ($x = 0$), we have computed the M -branch and the V -branch as shown in Fig. 14, which was already given in [1] up to level $L = 4$.⁶ In the theory of Q' with $x = -1$, we find the M -branch and the V -branch as shown in Fig. 15. In both cases,

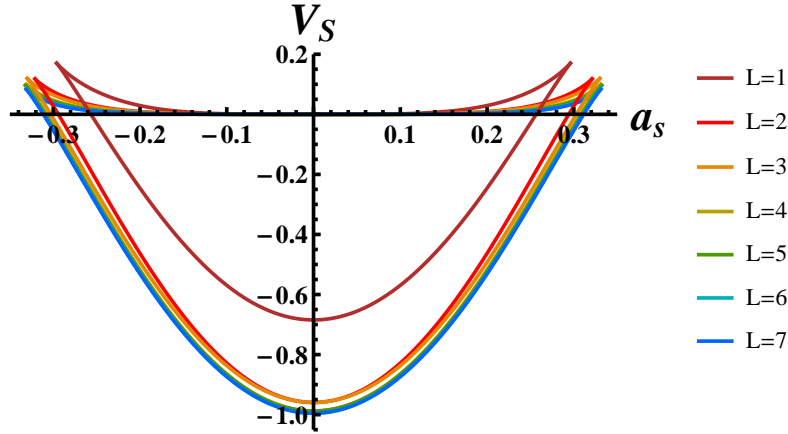


Figure 14: The M -branch and the V -branch in the Siegel gauge in the original theory ($x = 0$) with level $L = 1, 2, \dots, 7$ truncation.

with increasing level, the plots of the M -branch become flatter and it seems that there exist a maximum and minimum of the values of the massless field a_s , where the M -branch and the V -branch merge, for further higher levels. Comparing Fig. 15 with Fig. 14, the qualitative features of the graphs are similar, except that both branches move in the horizontal direction.

3.1 M - and V -branches for various values of x in $L = 6$

Here, we demonstrate the numerical results in the level $L = 6$ truncation.

For small values of $|x|$, we have plots of V -branches as in Fig. 16 and for large values of $|x|$, we have those in Fig. 17. In Fig. 16, the V -branch plot moves to the right in the horizontal

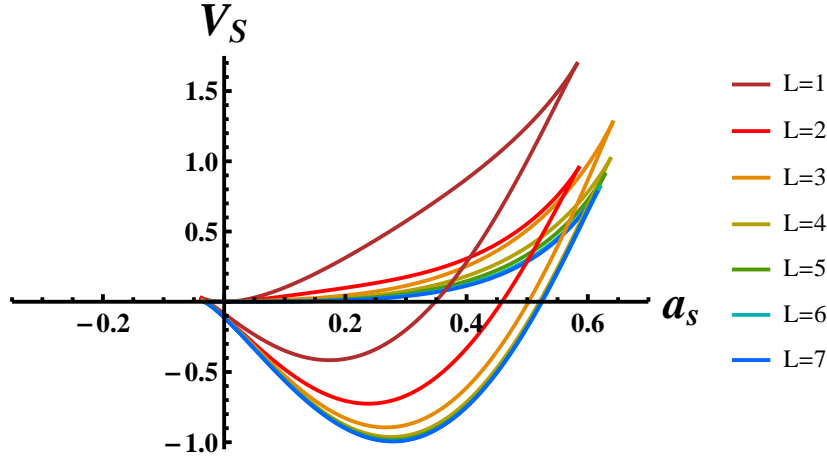


Figure 15: The M -branch and the V -branch in the Siegel gauge in the theory of $x = -1$ with level $L = 1, 2, \dots, 7$ truncation.

direction when the value of x changes from $x = 0$ to $x = -1.3$. Then, in Fig. 17, the left end of the V -branch remains near the origin (i.e. $a_s = 0$) and the potential minimum moves to the upper left when the value of x changes from $x = -1.4$ to $x = -3.6$. In the end, i.e. $x \simeq -3.6$, the V -branch is similar to the “ M -branch” in the sense that the plot appears to be flat around $a_s \gtrsim 0$.

On the other hand, for small values of $|x|$, we have plots of the M -branches as in Fig. 18 and for large values of $|x|$, we have those in Fig. 19. In Fig. 18, the M -branch plot moves to the right when the value of x changes from $x = 0$ to $x = -1.3$. Then, in Fig. 19, the left end of the V -branch remains near the origin and the value of the potential suddenly increases for positive values of a_s when the value of x changes from $x = -1.5$ to $x = -3.7$. In this sense, the M -branch seems to be unstable for $x < -1.4$.

3.2 On a bound of $|a_s|$

From the results so far, there seems to be a finite bound on the value of the massless field a_s for the numerical solutions in the Siegel gauge even in the theory of Q' with $x \neq 0$. Let us investigate the x -dependence of the value of a_s at the tachyon vacuum, which is the minimum in the V -branch, in the Siegel gauge. We have obtained the numerical result shown in Fig. 20. From Fig. 20, the plot seems to be convergent to a curve, which has a finite maximum of a_s , in the limit $L \rightarrow \infty$.

Actually, we can explain this x -dependence of a_s in the Siegel gauge as follows. We note that (2.9) and (2.10) can be rewritten as

$$b_0\Phi = 0, \quad L'\Phi + b_0(\Phi * \Phi) = 0, \quad (3.7)$$

⁶ Precisely speaking, the method of $(L, 2L)$ approximation instead of $(L, 3L)$ was performed in [1].

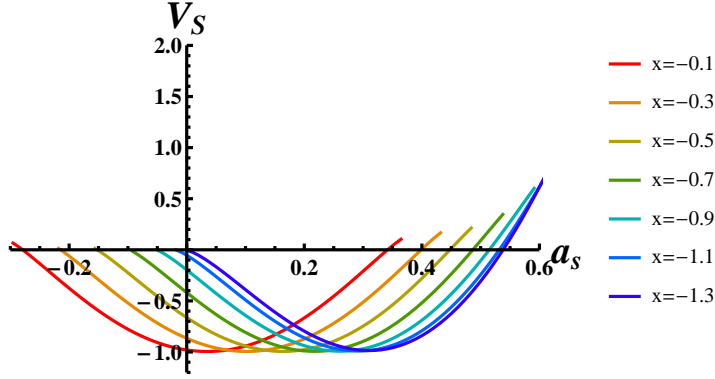


Figure 16: The V -branch in the Siegel gauge in the theory of Q' with $x = -0.1, -0.3, -0.5, \dots, -1.3$ with level $L = 6$ truncation.

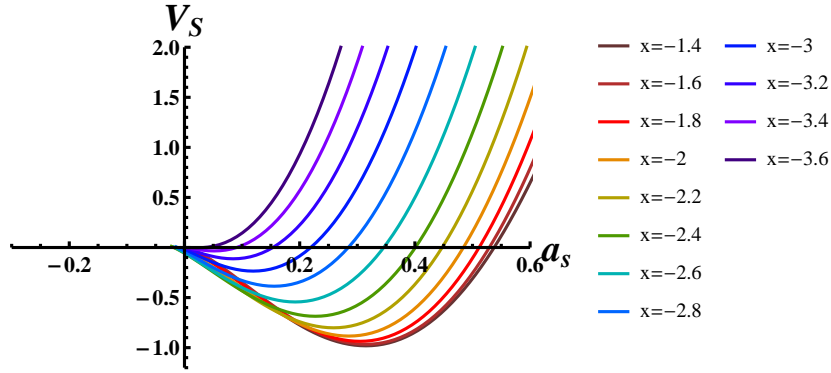


Figure 17: The V -branch in the Siegel gauge in the theory of Q' with $x = -1.4, -1.6, \dots, -3.6$ with level $L = 6$ truncation.

where L' can be expressed, using $U(x)$ such as $U(x)^\dagger = U(x)^{-1}$, as follows:

$$L' \equiv \{b_0, Q'\} = L_0 + \frac{x}{\sqrt{2}}(\alpha_{-1}^{25} + \alpha_1^{25}) + \frac{x^2}{2} = U(x)L_0U(x)^{-1}, \quad (3.8)$$

$$U(x) = \exp\left(\frac{x}{\sqrt{2}}(\alpha_1^{25} - \alpha_{-1}^{25})\right) = e^{-\frac{1}{4}x^2} \exp\left(-\frac{x}{\sqrt{2}}\alpha_{-1}^{25}\right) \exp\left(\frac{x}{\sqrt{2}}\alpha_1^{25}\right). \quad (3.9)$$

For any string fields A, B , we have

$$U(x)^{-1}(A * B) = (U(x)^{-1}A) * (U(x)^{-1}B) \quad (3.10)$$

and therefore the tachyon vacuum solutions Φ_x in the Siegel gauge in the theory of Q' with different values of x can be related as

$$\Phi_{x_2} = U(x_2)U(x_1)^{-1}\Phi_{x_1} = U(x_2 - x_1)\Phi_{x_1} \quad (3.11)$$

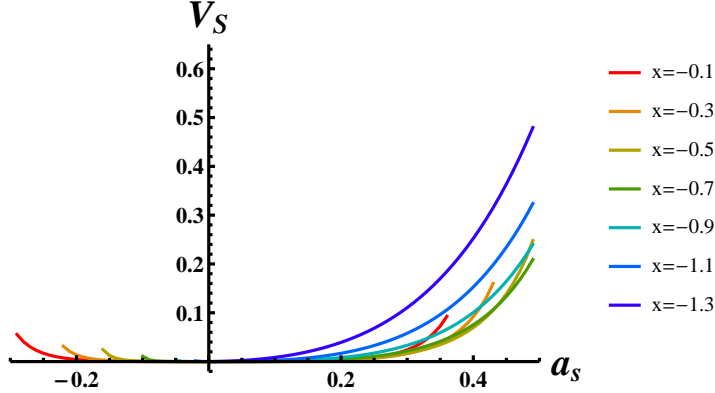


Figure 18: The M -branch in the Siegel gauge in the theory of Q' with $x = -0.1, -0.3, -0.5, \dots, -1.3$ with level $L = 6$ truncation.

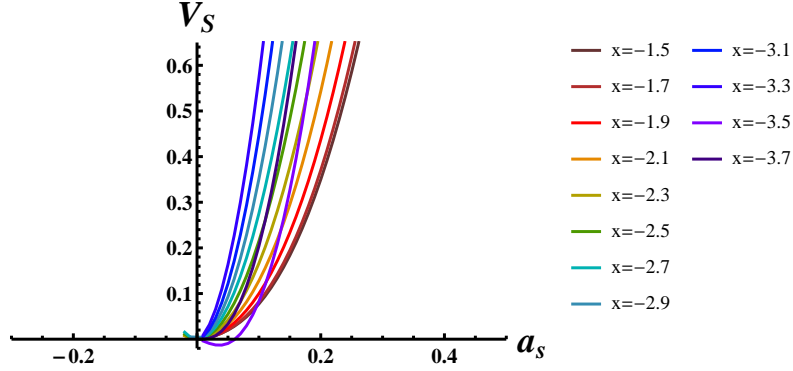


Figure 19: The M -branch in the Siegel gauge in the theory of Q' with $x = -1.5, -1.7, \dots, -3.7$ with level $L = 6$ truncation.

without the level truncation. Noting

$$\begin{aligned}
 U(x)(\alpha_{-1}^{25})^n c_1|0\rangle &= \left(\alpha_{-1}^{25} + \frac{x}{\sqrt{2}}\right)^n e^{-\frac{1}{4}x^2} \exp\left(-\frac{x}{\sqrt{2}}\alpha_{-1}^{25}\right) c_1|0\rangle \\
 &= e^{-\frac{1}{4}x^2} \left[\left(\frac{x}{\sqrt{2}}\right)^n c_1|0\rangle + \left(\frac{n}{\sqrt{2}}x - \left(\frac{x}{\sqrt{2}}\right)^{n+1}\right) \alpha_{-1}^{25} c_1|0\rangle + \dots \right], \quad (3.12)
 \end{aligned}$$

and using the expansion of the tachyon vacuum in the original theory ($x = 0$):

$$\Phi_0 = \sum_{m \geq 0} a_s^{(m)} (\alpha_{-1}^{25})^{2m} c_1|0\rangle + \dots, \quad (3.13)$$

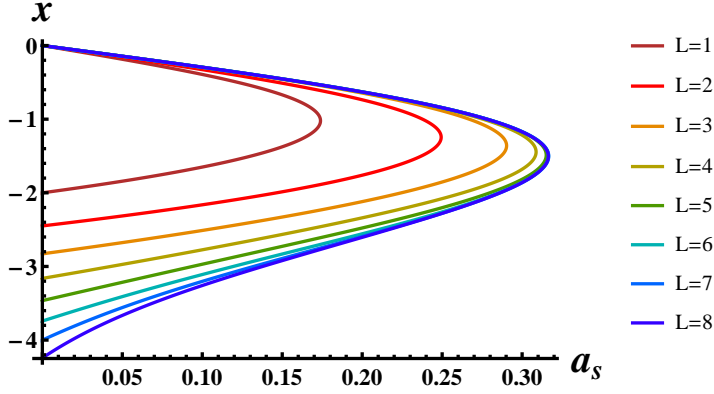


Figure 20: Plots of a_s as a function of x for the tachyon vacuum in the Siegel gauge using the numerical results in the level $L = 1, 2, \dots, 8$ truncation.

where we have used the fact that Φ_0 is twist even, we have

$$\begin{aligned} \Phi_x &= U(x)\Phi_0 \\ &= e^{-\frac{1}{4}x^2} \left[\sum_{m \geq 0} a_s^{(m)} \left(\frac{x}{\sqrt{2}} \right)^{2m} c_1|0\rangle + \sum_{m \geq 0} a_s^{(m)} \left(\sqrt{2}mx - \left(\frac{x}{\sqrt{2}} \right)^{2m+1} \right) \alpha_{-1}^{25} c_1|0\rangle + \dots \right]. \end{aligned} \quad (3.14)$$

Hence, if we do not truncate the level, the x -dependence of the tachyon field t_0 and the massless field a_s is given by

$$t_0 = e^{-\frac{1}{4}x^2} \sum_{m \geq 0} a_s^{(m)} \left(\frac{x}{\sqrt{2}} \right)^{2m}, \quad (3.15)$$

$$a_s = e^{-\frac{1}{4}x^2} \sum_{m \geq 0} a_s^{(m)} \left(\sqrt{2}mx - \left(\frac{x}{\sqrt{2}} \right)^{2m+1} \right). \quad (3.16)$$

It is necessary to know all coefficients $a_s^{(m)}$ ($m = 0, 1, 2, \dots$) in (3.13) in order to obtain the exact form of (3.16). However, this is impossible because no explicit expression of the exact solution in the Siegel gauge is yet known. Instead, let us use the level-truncated numerical solution in the original theory to obtain an approximate expression for (3.16). Such a function a_s with (3.16) can be compared to the plot using numerical data as given in Figs. 21, 22 and 23. (The left plot in each figure is from Fig. 20.) With increasing truncation level, the two plots get closer. These plots seem to imply that level truncation can be a good approximation to obtain a_s as a function of x using numerical data. If we use numerical configurations of the tachyon vacuum solution in the Siegel gauge in the original theory ($x = 0$), we obtain a_s of the form (3.16) as a function of x at each truncated level. Using these functions, we can see the maximum of a_s , $\max(a_s)$, and the value of x , x_{cr} , which give $\max(a_s)$, as in Figs. 24 and 25, respectively. With the numerical data up to $L = 26$ obtained in [18], we have extrapolated

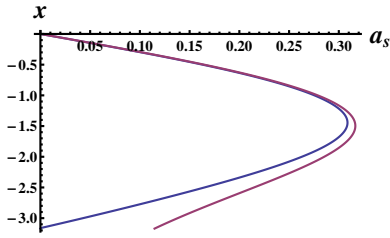


Figure 21: Plots of Fig. 20 and a_s given by (3.16) using numerical data in the level $L = 4$ truncation.

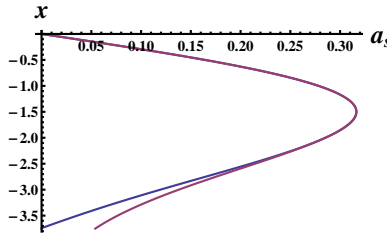


Figure 22: Plots of Fig. 20 and a_s given by (3.16) using numerical data in the level $L = 6$ truncation.

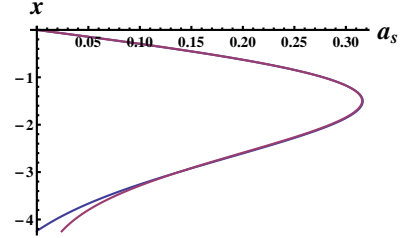


Figure 23: Plots of Fig. 20 and a_s given by (3.16) using numerical data in the level $L = 8$ truncation.

values for $L = \infty$: $\max(a_s) = 0.3118$ and $x_{\text{cr}} = -1.4986$, using a fitting function of the form $\sum_{k=0}^{13} c_k/L^k$. We note that both values are finite.

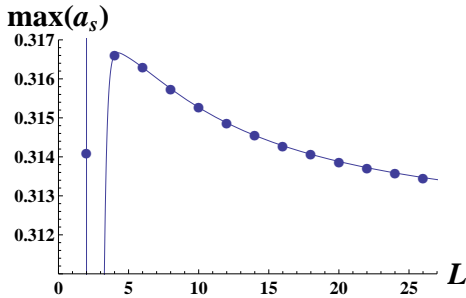


Figure 24: The maximum of a_s (3.16) using data in the truncation level $L = 2, 4, \dots, 26$ in the original theory. The solid line denotes the plot of a fitting function of the form $\sum_{k=0}^{13} c_k/L^k$.

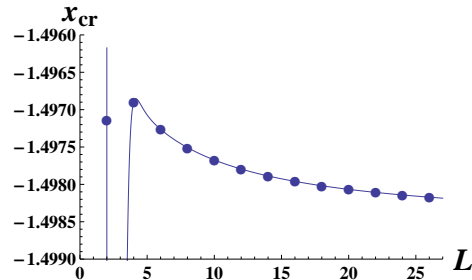


Figure 25: Plot of x_{cr} giving $\max(a_s)$ as in Fig. 24. The solid line denotes the plot of fitting function of the form $\sum_{k=0}^{13} c_k/L^k$.

4 On the gauge invariant overlaps of numerical solutions in the M -branch

In the original Q_B theory, the gauge invariant overlaps for the configurations of the M -branch Ψ_M in the Siegel gauge, which correspond to the upper branch for each truncation level in Fig. 14, are evaluated as Figs. 26, 27 and 28.

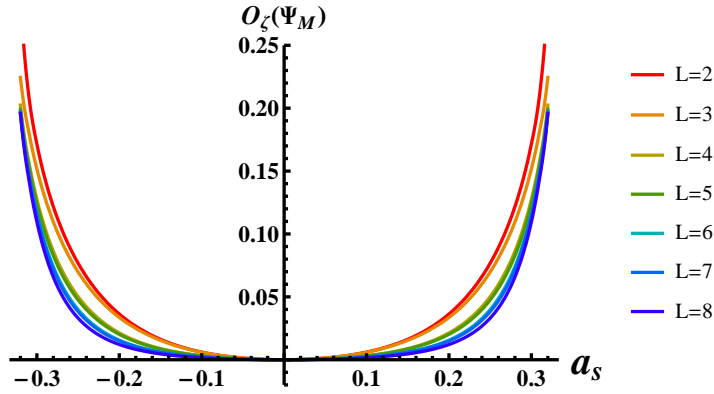


Figure 26: The gauge invariant overlap with the graviton for the M -branch in the Siegel gauge in the truncation level $L = 2, 3, \dots, 8$.

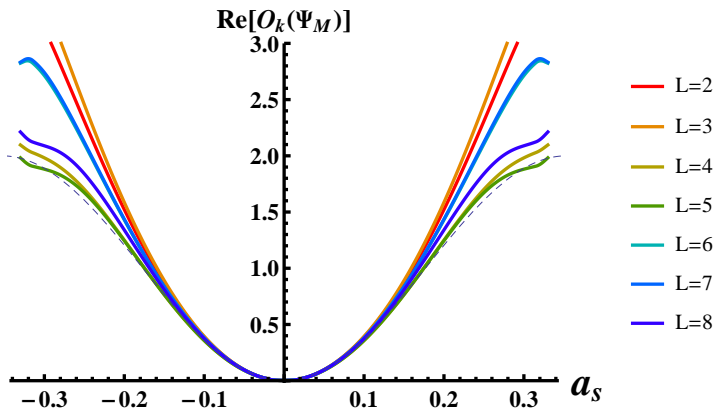


Figure 27: The real part of the gauge invariant overlap with the closed tachyon for the M -branch in the Siegel gauge in the truncation level $L = 2, 3, \dots, 8$. The dashed line shows $1 - \cos(\frac{4\pi}{\sqrt{2}}a_s)$.

From Fig. 26, we observe that $O_\zeta(\Psi_M)$ approaches 0 for a fixed value of a_s with increasing level. This result is consistent with Fig. 14 and the relation with the vacuum energy [19]. From Figs. 27 and 28, $\text{Re}(O_\zeta(\Psi_M))$ and $\text{Im}(O_\zeta(\Psi_M))$ nontrivially depend on a_s and *roughly* approach $1 - \cos(ca_s)$ and $\sin(ca_s)$, respectively with increasing level, where c is an appropriate constant.

Here, we would like to speculate on the possibility of a relationship between the above numerical result and the analytic result given in [20]. The identity-based marginal solution $\Psi_0(2.1)$ is expected to correspond to the numerical solution of the M -branch in the Siegel gauge. As for the parameter, the value of the massless field a_s corresponds to f given in (2.2). Let us consider the relationship to the parameter x , which is proportional to f , i.e. $f = (-2/\pi)x$, more explicitly. The massless field, or the coefficient of $\alpha_{-1}^{25}c_1|0\rangle$, is included

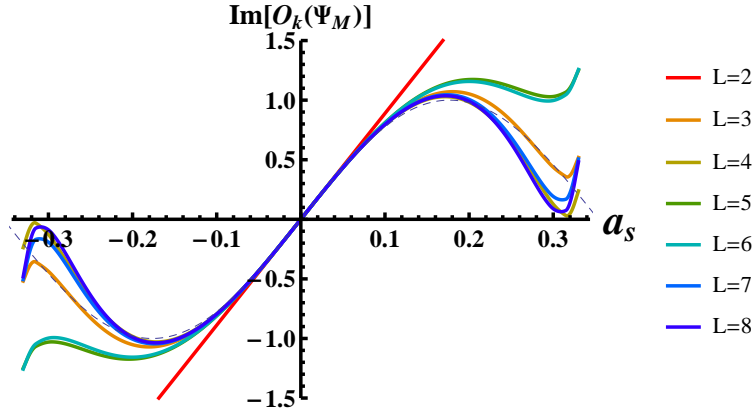


Figure 28: The imaginary part of the gauge invariant overlap with the closed tachyon for the M -branch in the Siegel gauge in the truncation level $L = 2, 3, \dots, 8$. The dashed line shows $\sin(\frac{4\pi}{\sqrt{2}}a_s)$.

only in the first term of $\Psi_0(2.1)$. We can expand it as follows:

$$\begin{aligned}
& - \int_{C_{\text{left}}} \frac{dz}{2\pi i} \frac{i}{2\sqrt{\alpha'}} F(z) c(z) \partial X^{25}(z) I = \frac{x}{\sqrt{2}} \int_{C_{\text{left}}} \frac{dz}{2\pi i} \frac{z + z^{-1}}{z} \sum_{n,m} c_n \alpha_m^{25} z^{-n-m} |I\rangle \\
& = \frac{x}{\sqrt{2}} \left(\frac{8}{3\pi} (c_1 + c_{-1}) + \sum_{k=1}^{\infty} \frac{2}{\pi} \left(\frac{1}{1-4k^2} - \frac{1}{1-4(k+1)^2} \right) (c_1 - c_{-1}) \right) \alpha_{-1}^{25} |I\rangle + \dots \\
& = \frac{\sqrt{2}}{\pi} x \alpha_{-1}^{25} c_1 |0\rangle + \dots, \tag{4.1}
\end{aligned}$$

where use has been made of the relations $\alpha_n^\mu |I\rangle = -(-1)^n \alpha_{-n}^\mu |I\rangle$ and $(c_{2k+1} - c_{-2k-1}) |I\rangle = (-1)^k (c_1 - c_{-1}) |I\rangle$. Therefore, we expect the correspondence of the parameters between the solutions to the original theory to be $a_s \sim (\sqrt{2}/\pi)x$.

In this context, we may expect that the numerical solution with the parameter a_s , which we denote as $\Psi_M(a_s)$, is gauge equivalent to the identity-based marginal solution $\Psi_0(x)$ (2.1) with the parameter $x \simeq (\pi/\sqrt{2})a_s$. If this expectation is valid, the gauge invariant overlap for them should be

$$O_V(\Psi_M(a_s)) \simeq O_V(\Psi_0(x = (\pi/\sqrt{2})a_s)). \tag{4.2}$$

On the right-hand side of the above equation, from the result in [20], we have $O_\zeta(\Psi_0(x)) = 0$ for the graviton and $O_k(\Psi_0(x)) = 1 - e^{-4ix}$ for the closed tachyon, which are roughly consistent with the numerical results in Figs. 26, 27 and 28. Here, we should note that the parameter x in Ψ_0 does not have a finite bound and we can take any large value of $|x|$ from the viewpoint of the solution to the equation of motion. However, the parameter a_s seems to have a finite bound and we can take a_s only in $|a_s| \lesssim 0.3$ as is seen from Fig. 14. In this sense, the assumption $x \simeq (\pi/\sqrt{2})a_s$ cannot be justified for large values of $|a_s|$ such as $|a_s| > 0.3$. Therefore, we do not have a definite conclusion on the gauge equivalence between the M -branch numerical solution and the identity-based marginal solution Ψ_0 .

5 Concluding remarks

We have constructed numerical solutions using the conventional level truncation method in the theory of Q' obtained by expanding the string field around an identity-based marginal solution, which has one parameter, x :

(a) We have constructed tachyon vacuum solutions in the Siegel gauge and the Landau gauge. With increasing level, the values of the action at the solutions approach a D-brane tension in the wider range of the parameter x . This suggests that the energy of the identity-based marginal solution vanishes as in the case of the solution with $K'Bc$ algebra [9], which satisfies the other gauge condition.

(b) We have constructed the M -branch and the V -branch in the theories of various values of x in the Siegel gauge. The values of the potential approach zero for higher levels for small values of the massless field $|a_s|$ in the M -branch and the potential form roughly moves in the horizontal direction according to the values of x . However, it turns out that there seems to exist a finite bound for the value of the massless field a_s in the theory of Q' with any value of x as in the original theory of Q_B ($x = 0$), which was observed in previous work [1].

(c) We have evaluated the gauge invariant overlaps with the graviton and the closed tachyon for the constructed numerical solutions. For the numerical tachyon vacuum solution, they approach the same x -dependence as the analytic ones [9] with increasing truncation level.

For the numerical tachyon vacuum solutions Φ_x in the Siegel gauge, we have checked the remaining part of the equation of motion (or the BRST invariance of the gauge fixed solutions) for consistency in appendix A. As the truncation level is increased, the vacuum energy E of Φ_x , which is normalized by a D-brane tension, seems to become -1 for *any* value of x , as in Fig. 1. Actually, this can be justified as follows. Without level truncation, the solution in the Siegel Φ_x can be related to the tachyon vacuum solution in the Siegel Φ_0 in the original Q_B theory ($x = 0$) as $\Phi_x = U(x)\Phi_0$ (3.14). Noting the relations involving $U(x)$, (3.8) and (3.10), we find that the value of the action (2.3) does not depend on x , namely, $S'[\Phi_x] = S[\Phi_0]$. Additionally, it is well confirmed that the normalized vacuum energy of Φ_0 should be -1 using the level truncation method. In a similar manner, we can justify our numerical evidence of $O_\zeta(\Phi_x) = 1$ and $O_k(\Phi_x) = e^{-4ix}$ in §2.3: Without the level truncation, we can show that $O_\zeta(U(x)\Phi_0) = O_\zeta(\Phi_0)$ and $O_k(U(x)\Phi_0) = e^{-4ix}O_k(\Phi_0)$ using explicit expression of the gauge invariant overlap. Then, we have the equality $O_\zeta(\Phi_0) = O_k(\Phi_0)$ [16] and its value should be 1, as was numerically checked in [18].

Acknowledgements

The work of I. K. and T. T. is supported by a JSPS Grant-in-Aid for Scientific Research (B) (#24340051). The work of I. K. is supported in part by a JSPS Grant-in-Aid for Young Scientists (B) (#25800134). The work of I. K. was supported partly by a Grant for Promotion of Niigata University Research Projects and partly by a Grant-in-Aid for Research Project from Institute of Humanities, Social Sciences and Education, Niigata University. The numerical computation in this work was partly carried out at the Yukawa Institute Computer Facility.

A On the BRST invariance of the numerical solutions

We have constructed numerical solutions to eqs. (2.9) and (2.10). However, initially, we would like to construct the solution to the equation of motion $Q'\Phi + \Phi * \Phi = 0$. Therefore, as a consistency check, we evaluate the remaining part of the equation of motion, namely,

$$\text{bpz}(\mathcal{P}_1)(Q'\Phi + \Phi * \Phi) = 0, \quad (\text{A.1})$$

which corresponds to the BRST invariance of the gauge fixed solution [21]. In the case of the Siegel gauge, we have $\text{bpz}(\mathcal{P}_1) = b_0 c_0$ and we evaluate

$$\frac{\|b_0 c_0(Q'\Phi + \Phi * \Phi)\|}{\|\Phi\|}, \quad (\text{A.2})$$

numerically. In the above, the norms of string fields with ghost number 1 in the denominator and ghost number 2 in the numerator are defined for an orthonormalized basis with respect to the BPZ inner product as in [15]. For the numerical solutions to eqs. (2.9) and (2.10) in the Siegel gauge, which correspond to Fig. 1, the ratio of norms (A.2) is evaluated as Fig. 29. Roughly speaking, the value of (A.2) remains “small” with increasing truncation

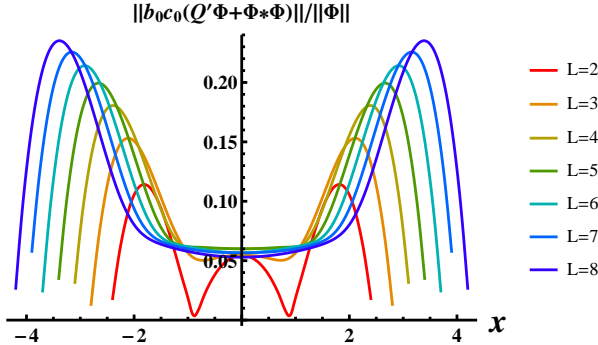


Figure 29: Plots of (A.2) in the level $L = 2, 3, \dots, 8$ truncation.

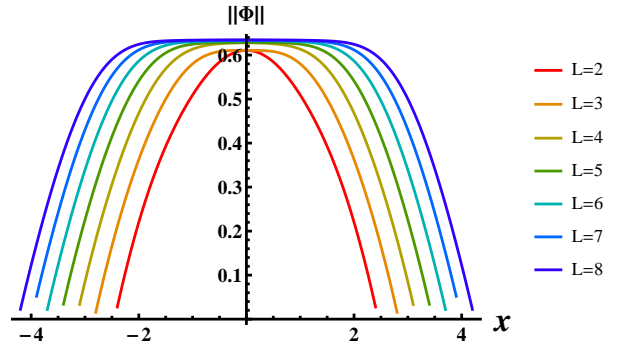


Figure 30: Plots of $\|\Phi\|$ in Fig. 29 in the level $L = 2, 3, \dots, 8$ truncation.

level. Although there are peaks for large $|x|$ in each plot in Fig. 29, they are related to the decline of the denominator of (A.2), i.e., the norm of the configuration $\|\Phi\|$, as in Fig. 30. Next, let us see the coefficient of $c_{-2}c_1|0\rangle$ in $b_0 c_0(Q'\Phi + \Phi * \Phi)$ as one of the component fields.

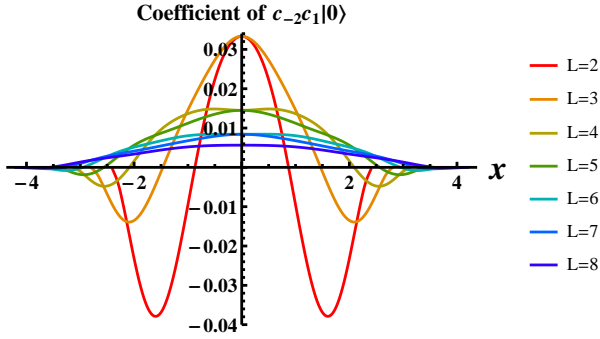


Figure 31: Plots of the coefficient of $c_{-2}c_1|0\rangle$ in $b_0c_0(Q'\Phi + \Phi * \Phi)$ in the level $L = 2, 3, \dots, 8$ truncation.

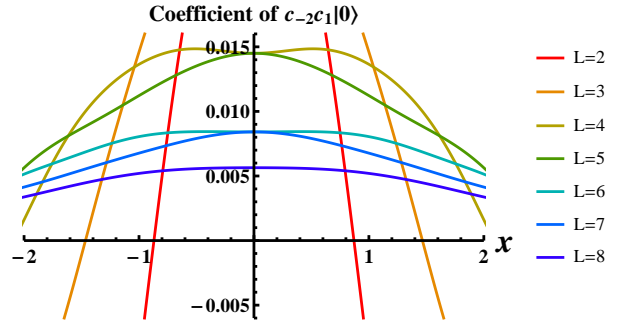


Figure 32: Enlargement of Fig. 31

From Figs. 31 and 32, the coefficient of $c_{-2}c_1|0\rangle$ gets closer to zero as the truncation level increases for each value of x . Therefore, we expect that all coefficients of $b_0c_0(Q'\Phi + \Phi * \Phi)$ approach zero in infinite level limit, although the norm convergence might be slow.

The above results imply that our numerical solutions to eqs. (2.9) and (2.10), which correspond to Fig. 1, can be consistently regarded as approximate solutions to the equation of motion $Q'\Phi + \Phi * \Phi = 0$.

References

- [1] A. Sen and B. Zwiebach, “Large marginal deformations in string field theory,” JHEP **0010**, 009 (2000) [arXiv:hep-th/0007153].
- [2] T. Takahashi and S. Tanimoto, “Wilson lines and classical solutions in cubic open string field theory,” Prog. Theor. Phys. **106**, 863 (2001) [arXiv:hep-th/0107046].
- [3] T. Takahashi and S. Tanimoto, “Marginal and scalar solutions in cubic open string field theory,” JHEP **0203**, 033 (2002) [arXiv:hep-th/0202133].
- [4] I. Kishimoto and T. Takahashi, “Marginal deformations and classical solutions in open superstring field theory,” JHEP **0511**, 051 (2005) [arXiv:hep-th/0506240].
- [5] M. Schnabl, “Comments on marginal deformations in open string field theory,” Phys. Lett. B **654**, 194 (2007) [hep-th/0701248 [HEP-TH]].
- [6] M. Kiermaier, Y. Okawa, L. Rastelli and B. Zwiebach, “Analytic solutions for marginal deformations in open string field theory,” JHEP **0801**, 028 (2008) [hep-th/0701249 [HEP-TH]].
- [7] E. Fuchs, M. Kroyter and R. Potting, “Marginal deformations in string field theory,” JHEP **0709**, 101 (2007) [arXiv:0704.2222 [hep-th]].

- [8] M. Kiermaier and Y. Okawa, “Exact marginality in open string field theory: A General framework,” JHEP **0911**, 041 (2009) [arXiv:0707.4472 [hep-th]].
- [9] S. Inatomi, I. Kishimoto and T. Takahashi, “Tachyon Vacuum of Bosonic Open String Field Theory in Marginally Deformed Backgrounds,” PTEP **2013**, 023B02 (2013) [arXiv:1209.4712 [hep-th]].
- [10] M. Kudrna, T. Masuda, Y. Okawa, M. Schnabl and K. Yoshida, “Gauge-invariant observables and marginal deformations in open string field theory,” JHEP **1301**, 103 (2013) [arXiv:1207.3335 [hep-th]].
- [11] T. Erler and M. Schnabl, “A Simple Analytic Solution for Tachyon Condensation,” JHEP **0910**, 066 (2009) [arXiv:0906.0979 [hep-th]].
- [12] M. Asano and M. Kato, “New Covariant Gauges in String Field Theory,” Prog. Theor. Phys. **117**, 569 (2007) [hep-th/0611189].
- [13] M. Asano and M. Kato, “General Linear Gauges and Amplitudes in Open String Field Theory,” Nucl. Phys. B **807**, 348 (2009) [arXiv:0807.5010 [hep-th]].
- [14] M. Asano and M. Kato, “Level Truncated Tachyon Potential in Various Gauges,” JHEP **0701**, 028 (2007) [hep-th/0611190].
- [15] I. Kishimoto and T. Takahashi, “Numerical Evaluation of Gauge Invariants for a -gauge Solutions in Open String Field Theory,” Prog. Theor. Phys. **121**, 695 (2009) [arXiv:0902.0445 [hep-th]].
- [16] T. Kawano, I. Kishimoto and T. Takahashi, “Gauge Invariant Overlaps for Classical Solutions in Open String Field Theory,” Nucl. Phys. B **803**, 135 (2008) [arXiv:0804.1541 [hep-th]].
- [17] S. Inatomi, I. Kishimoto and T. Takahashi, “On nontrivial solutions around a marginal solution in cubic superstring field theory,” JHEP **1212**, 071 (2012) [arXiv:1209.6107 [hep-th]].
- [18] I. Kishimoto, “On numerical solutions in open string field theory,” Prog. Theor. Phys. Suppl. **188**, 155 (2011).
- [19] T. Baba and N. Ishibashi, “Energy from the gauge invariant observables,” JHEP **1304**, 050 (2013) [arXiv:1208.6206 [hep-th]].
- [20] I. Kishimoto and T. Takahashi, “Gauge invariant overlaps for identity-based marginal solutions,” *to appear*.
- [21] H. Hata and S. 'i. Shinohara, “BRST invariance of the nonperturbative vacuum in bosonic open string field theory,” JHEP **0009**, 035 (2000) [hep-th/0009105].